Physics Letters B 702 (2011) 324–328

Contents lists available at ScienceDirect

Physics Letters B

www.elsevier.com/locate/physletb

Observation of the rare $\eta \to e^+e^-e^+e^-$ decay with the KLOE experiment

KLOE Collaboration

F. Ambrosino [d,e], A. Antonelli [a], M. Antonelli [a], F. Archilli [i,j], I. Balwierz [b], G. Bencivenni [a], C. Bini [g,h], C. Bloise [a], S. Bocchetta [k,l], F. Bossi [a], P. Branchini [l], G. Capon [a], T. Capussela [a], F. Ceradini [k,l], P. Ciambrone [a], E. Czerwiński [a], E. De Lucia [a], A. De Santis [g,h], P. De Simone [a], G. De Zorzi [g,h], A. Denig [c], A. Di Domenico [g,h], C. Di Donato [e], B. Di Micco [k,l], M. Dreucci [a], G. Felici [a], S. Fiore [g,h], P. Franzini [g,h], C. Gatti [a], P. Gauzzi [g,h], S. Giovannella [a,*], E. Graziani [l], M. Jacewicz [a], J. Lee-Franzini [a,m], M. Martemianov [o], M. Martini [a,f,1], P. Massarotti [d,e], S. Meola [d,e], S. Miscetti [a], G. Morello [a], M. Moulson [a], S. Müller [c], M. Napolitano [d,e], F. Nguyen [k,l], M. Palutan [a], A. Passeri [l], V. Patera [a,f], I. Prado Longhi [k,l], P. Santangelo [a], B. Sciascia [a], M. Silarski [b], T. Spadaro [a], C. Taccini [k,l], L. Tortora [l], G. Venanzoni [a], R. Versaci [a,f,*,2], G. Xu [a,n], J. Zdebik [b]

and, as members of the KLOE-2 Collaboration:

D. Babusci [a], D. Badoni [i,j], V. Bocci [h], A. Budano [k,l], S.A. Bulychjev [o], P. Campana [a], E. Dané [a], G. De Robertis [q], D. Domenici [a], O. Erriquez [p,q], G. Fanizzi [p,q], F. Gonnella [i,j], F. Happacher [a], B. Höistad [t], E. Iarocci [f,a], T. Johansson [t], V. Kulikov [o], A. Kupsc [t], F. Loddo [q], M. Matsyuk [o], R. Messi [i,j], D. Moricciani [j], P. Moskal [b], A. Ranieri [q], I. Sarra [a], M. Schioppa [r,s], A. Sciubba [f,a], W. Wiślicki [u], M. Wolke [t]

[a] *Laboratori Nazionali di Frascati dell'INFN, Frascati, Italy*
[b] *Institute of Physics, Jagiellonian University, Krakow, Poland*
[c] *Institut für Kernphysik, Johannes Gutenberg – Universität Mainz, Germany*
[d] *Dipartimento di Scienze Fisiche dell'Università "Federico II", Napoli, Italy*
[e] *INFN Sezione di Napoli, Napoli, Italy*
[f] *Dipartimento di Scienze di Base ed Applicate per l'Ingegneria dell'Università "Sapienza", Roma, Italy*
[g] *Dipartimento di Fisica dell'Università "Sapienza", Roma, Italy*
[h] *INFN Sezione di Roma, Roma, Italy*
[i] *Dipartimento di Fisica dell'Università "Tor Vergata", Roma, Italy*
[j] *INFN Sezione di Roma Tor Vergata, Roma, Italy*
[k] *Dipartimento di Fisica dell'Università "Roma Tre", Roma, Italy*
[l] *INFN Sezione di Roma Tre, Roma, Italy*
[m] *Physics Department, State University of New York at Stony Brook, USA*
[n] *Institute of High Energy Physics of Academica Sinica, Beijing, China*
[o] *Institute for Theoretical and Experimental Physics, Moscow, Russia*

and

[p] *Dipartimento di Fisica dell'Università di Bari, Bari, Italy*
[q] *INFN Sezione di Bari, Bari, Italy*
[r] *Dipartimento di Fisica dell'Università della Calabria, Cosenza, Italy*
[s] *INFN Gruppo collegato di Cosenza, Cosenza, Italy*
[t] *Department of Nuclear and Particle Physics, Uppsala Univeristy, Uppsala, Sweden*
[u] *A. Soltan Institute for Nuclear Studies, Warsaw, Poland*

* Corresponding authors.
E-mail addresses: simona.giovannella@lnf.infn.it (S. Giovannella), roberto.versaci@lnf.infn.it (R. Versaci).
[1] Present address: Dipartimento di Scienze e Tecnologie Applicate, Università Guglielmo Marconi, Roma, Italy.
[2] Present address: CERN, CH-1211 Geneva 23, Switzerland.

0370-2693/$ – see front matter
doi:10.1016/j.physletb.2011.07.033

ARTICLE INFO

Article history:
Received 30 May 2011
Received in revised form 24 June 2011
Accepted 13 July 2011
Available online 22 July 2011
Editor: M. Doser

Keywords:
e^+e^- collisions
Rare η decays

ABSTRACT

We report the first observation of the rare $\eta \to e^+e^-e^+e^-(\gamma)$ decay based on 1.7 fb^{-1} collected by the KLOE experiment at the DAΦNE ϕ-factory. The selection of the $e^+e^-e^+e^-$ final state is fully inclusive of radiation. We have identified 362 ± 29 events resulting in a branching ratio of $(2.4 \pm 0.2_{stat+bckg} \pm 0.1_{syst}) \times 10^{-5}$.

1. Introduction

The $\eta \to e^+e^-e^+e^-$ decay proceeds through two virtual photons intermediate state with internal photon conversion to e^+e^- pairs. Conversion decays offer the possibility to precisely measure the virtual photon 4-momentum via the invariant mass of the e^+e^- pair. The lack of hadrons among the decay products makes the matrix element directly sensitive to the η meson transition form factor [1]. The knowledge of the η meson coupling to virtual photons is important for the calculation of the anomalous magnetic moment of the muon, being pseudoscalar exchange the major contribution to the hadronic light-by-light scattering.

The first theoretical evaluation, $\Gamma(\eta \to e^+e^-e^+e^-)/\Gamma(\eta \to \gamma\gamma) = 6.6 \times 10^{-5}$, dates from 1967 [2]. The width ratio translates into a branching ratio (BR) $\mathrm{BR}(\eta \to e^+e^-e^+e^-) = 2.59 \times 10^{-5}$ when the world average of the $\mathrm{BR}(\eta \to \gamma\gamma)$ measurements [3] is taken as normalization factor. Other predictions exist in literature [4–7], with differences at the level of 10%.

Double lepton–antilepton η decays have been searched by the CMD-2 and the WASA experiments, obtaining the upper limits at 90% C.L., $\mathrm{BR}(\eta \to e^+e^-e^+e^-) < 6.9 \times 10^{-5}$ [8] and $\mathrm{BR}(\eta \to e^+e^-e^+e^-) < 9.7 \times 10^{-5}$ [9], respectively.

2. The KLOE detector

The KLOE experiment operates at DAΦNE, the Frascati ϕ-factory. DAΦNE is an e^+e^- collider running at a center of mass energy of ~ 1020 MeV, the mass of the ϕ meson. Equal energy positron and electron beams collide at an angle of $\pi - 25$ mrad, producing nearly at rest ϕ mesons.

The detector consists of a large cylindrical Drift Chamber (DC), surrounded by a lead-scintillating fiber electromagnetic calorimeter. A superconducting coil around the EMC provides a 0.52 T field. The beam pipe at the interaction region is spherical in shape with 10 cm radius, it is made of a beryllium–aluminum alloy of 0.5 mm thickness. Low beta quadrupoles are located at about ±50 cm distance from the interaction region. The drift chamber [10], 4 m in diameter and 3.3 m long, has 12,582 all-stereo tungsten sense wires and 37,746 aluminum field wires. The chamber shell is made of carbon fiber-epoxy composite with an internal wall of 1.1 mm thickness, the gas used is a 90% helium, 10% isobutane mixture. The spatial resolutions are $\sigma_{xy} \sim 150$ μm and $\sigma_z \sim 2$ mm. The momentum resolution is $\sigma(p_\perp)/p_\perp \approx 0.4\%$. Vertices are reconstructed with a spatial resolution of ~ 3 mm. The calorimeter [11] is divided into a barrel and two endcaps, for a total of 88 modules, and covers 98% of the solid angle. The modules are read out at both ends by photomultipliers, both in amplitude and time. The readout granularity is $\sim (4.4 \times 4.4)$ cm^2, for a total of 2440 cells arranged in five layers. The energy deposits are obtained from the signal amplitude while the arrival times and the particles positions are obtained from the time differences. Cells close in time and space are grouped into calorimeter clusters. The cluster energy E is the sum of the cell energies. The cluster time T and position $\vec{R}$ are energy-weighted averages. Energy and time resolutions are $\sigma_E/E = 5.7\%/\sqrt{E(\mathrm{GeV})}$ and $\sigma_t = 57$ ps$/\sqrt{E(\mathrm{GeV})} \oplus 100$ ps, respectively. The trigger [12] uses both calorimeter and chamber information. In this analysis the events are selected by the calorimeter trigger, requiring two energy deposits with $E > 50$ MeV for the barrel and $E > 150$ MeV for the endcaps. A cosmic veto rejects events with at least two energy deposits above 30 MeV in the outermost calorimeter layer. Data are then analyzed by an event classification filter [13], which selects and streams various categories of events in different output files.

3. Event selection

The analysis has been performed using 1733 pb^{-1} from the 2004–2005 data set at $\sqrt{s} \simeq 1.02$ GeV. 242 pb^{-1} of data taken off-peak at $\sqrt{s} = 1.0$ GeV were used to study the e^+e^- continuum. Monte Carlo (MC) events are used to simulate the signal and the background. The signal is generated according to the matrix element in [5], assuming $\mathrm{BR} = 2.7 \times 10^{-5}$, in a sample of 167,531 pb^{-1}. Other MC samples are: 3447 pb^{-1} simulating the main ϕ decays ($\phi \to K\bar{K}$ and $\phi \to \rho\pi$) and 17,517 pb^{-1} simulating others more rare ϕ decays. All MC productions account for run by run variations of the main data-taking parameters such as background conditions, detector response and beam configuration. Data-MC corrections for calorimeter cluster energies and tracking efficiency, evaluated with radiative Bhabha events and $\phi \to \rho\pi$ samples respectively, have been applied. Effects of Final State Radiation (FSR) have been taken into account using the PHOTOS MC package [14,15]. This package simulates the emission of FSR photons by any of the decay products taking also into account the interference between different diagrams. PHOTOS is used in the Monte Carlo at the event generation level, so that our simulation fully accounts for radiative effects.

At KLOE, η mesons are produced together with a monochromatic recoil photon ($E_\gamma = 363$ MeV) through the radiative decay $\phi \to \eta\gamma$. In the considered data sample about 72×10^6 η's are produced. As first step of the analysis, a preselection is performed requiring at least four (two positive and two negative) tracks extrapolated inside a fiducial volume defined by a cylinder centered in the interaction point and having radius $R = 4$ cm and length $\Delta z = 20$ cm. For each charge, the two tracks with the highest momenta are selected. One and only one neutral cluster, having energy $E_{cl} \geqslant 250$ MeV and polar angle in the range (23°–157°), is required. A cluster is defined neutral if it does not have any associated track and has a time of flight compatible with the photon hypothesis. To improve the energy and momentum resolution, a kinematic fit is performed imposing the four-momentum conservation and the photon time of flight. A very loose cut on the χ^2 of

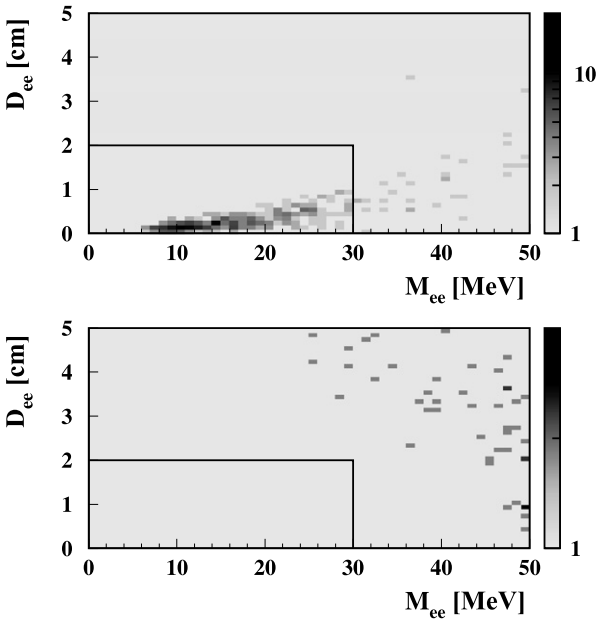

Fig. 1. D_{ee} vs M_{ee} evaluated at the drift chamber wall for MC $\phi \to \eta\gamma$ background (top panel) and MC signal (bottom panel). Events in the box $M_{ee}(DCW) < 30$ MeV $\cap$ $D_{ee}(DCW) < 2$ cm are rejected.

the kinematic fit ($\chi^2 < 4000$) is applied in order to discard poorly reconstructed events.

4. Background rejection

Two sources of background are present:

1. ϕ background:
   This is mainly due to $\phi \to \pi^+\pi^-\pi^0$ events (with π^0 Dalitz decay) and to $\phi \to \eta\gamma$ events either with $\eta \to \pi^+\pi^-\pi^0$ (with π^0 Dalitz decay) or $\eta \to \pi^+\pi^-e^+e^-$ or with $\eta \to e^+e^-\gamma$ (with photon conversion on the Beam Pipe, BP, or the DC inner Wall, DCW). This last background has the same signature of the signal. Background from $\phi \to K\bar{K}$ is also present at the preselection level.
2. e^+e^- continuum background:
   This is mainly due to $e^+e^- \to e^+e^-(\gamma)$ events with photon conversions, split tracks or interactions in the DAΦNE low beta quadrupoles. This background has been studied using off-peak data taken at $\sqrt{s} = 1$ GeV, where ϕ decays are negligible.

A first background rejection is performed cutting on the sum of the absolute value of the momenta of the four selected tracks requiring ($600 < \sum_1^4 |\vec{p}_i| < 700$) MeV.

To remove e^+e^- continuum background from interactions in the low beta quadrupoles, the quantities $\langle\cos\theta_f\rangle$ and $\langle\cos\theta_b\rangle$ have been defined as the average polar angle of forward and backward selected particles. Events having $\langle\cos\theta_f\rangle > 0.85$ and $\langle\cos\theta_b\rangle < -0.85$ are rejected. This cut has no effect on signal selection efficiency.

To reject events due to photon conversion, each track is extrapolated backward to the intersection with the BP and with the DCW. For each track pair, the invariant mass (M_{ee}) and the relative distance (D_{ee}) are computed. A clear signal of photon conversion is visible in the D_{ee}–M_{ee} 2D plot for BP and DCW (Fig. 1). Events having at least one combination satisfying $M_{ee}(BP) < 10$ MeV and $D_{ee}(BP) < 2$ cm or $M_{ee}(DCW) < 30$ MeV and $D_{ee}(DCW) < 2$ cm are rejected.

The last rejection is based on the Particle IDentification (PID) of charged particles. For each track associated to a calorimeter cluster, the quantity $\Delta t = t_{track} - t_{cluster}$ in both electron and pion hypothesis is evaluated; t_{track} is defined as the length of the track divided by $\beta(m)c$. Track with $\Delta t_e/\Delta t_\pi < 1 (> 1)$ are identified as electron (pion). Events having more than two pions or no electrons are discarded.

The effects of background rejection cuts on the various data components are visible in Fig. 2, where the four electrons invariant mass, $M_{e^+e^-e^+e^-}$, is shown at different steps of the analysis. In Table 1, number of events in data, N(data), MC signal efficiencies, ε(sig), and background rejection factor R, defined as the ratio of analysis efficiency between signal and background, are also reported. The R value has been evaluated for three different categories: $\phi \to \eta\gamma$ with $\eta \to e^+e^-\gamma$ ($R_{\eta\to e^+e^-\gamma}$), $\phi \to K\bar{K}$ and $\phi \to \rho\pi$ ($R_{\phi\to K\bar{K}/\rho\pi}$) and all other ϕ decays products (R_{others}). After all cuts, background from kaons and $\phi \to \pi^+\pi^-\pi^0$ events is negligible. The same holds for all other ϕ decays but $\eta \to e^+e^-\gamma$ which, as will be shown in the next section, results in $\sim 15\%$ contamination level. Systematics on the Monte Carlo description of photon conversion have been studied using events with similar characteristics. A clean control sample is provided by the $\phi \to \eta e^+e^-$, $\eta \to \pi^+\pi^-\pi^0$ decay chain, where simple analysis cuts provide a good data-MC agreement, with negligible background contamination. As for the $\eta \to e^+e^-e^+e^-$ channel, before dedicated analysis cuts the control sample is significantly contaminated by background from photon conversion ($\phi \to \eta\gamma$ with photon converting on beam pipe or drift chamber walls). This background is completely removed rejecting events with $D_{ee}(DCW) < 10$ cm and $M_{ee}(DCW) < 80$ MeV. For the $\eta \to e^+e^-e^+e^-$ channel this cut has not been applied because, having two electrons and two positrons in the final state, the search for a conversion has to be performed over all the four e^+e^- combinations, thus spreading the signal contribution in the $M_{ee}(DCW)$–$D_{ee}(DCW)$ plane and lowering significantly the analysis efficiency. Removing the cuts on M_{ee}–D_{ee} planes in the control sample, a clear background contamination from photon conversion is visible. Data-MC comparison shows that, increasing in the simulation the probability of conversion by 10%, an excellent agreement is found. A 10% systematic error is then assigned to photon conversion and added to the uncertainties coming from MC statistics and BR($\eta \to e^+e^-\gamma$) measurement [3]: $N(\eta \to e^+e^-\gamma) = 80 \pm 3_{\text{MC}} \pm 8_{\text{BR}} \pm 8_{syst}$.

5. Evaluation of the BR($\eta \to e^+e^-e^+e^-(\gamma)$)

As discussed in the previous section, the only significant background contamination surviving all the analysis cuts is due to $\eta \to e^+e^-\gamma$ events with photon conversion, that have a signature similar to the signal. The overall estimated background from ϕ decays has been subtracted bin-by-bin to the $M_{e^+e^-e^+e^-}$ spectrum obtained in data (Fig. 3 top), taking into account also systematic errors. The event counting is done fitting the resulting spectrum with the two residual contributions: signal and e^+e^- continuum background events. The $M_{e^+e^-e^+e^-}$ shape for the signal is obtained by fitting MC events with two Gaussian functions plus a third order polynomial function. The fit range is $500 < M_{e^+e^-e^+e^-} < 600$ MeV. The $M_{e^+e^-e^+e^-}$ distribution for e^+e^- continuum events has been studied on the data taken at $\sqrt{s} = 1$ GeV, where contributions from ϕ decays are suppressed. Even though the small statistics of the sample does not allow to precisely extract the shape, a first order polynomial well reproduces the data in the signal region. The free parameters are an overall scale factor for signal and the two parameters describing the e^+e^- continuum background. Fit results are shown in Fig. 3 bottom. The resulting χ^2/ndf is 43.9/34,

Table 1
Number of events in data, MC signal efficiency, background rejection factor at different steps of the analysis.

Cut	N(data)	ε(sig)	$R_{\eta\to e^+e^-\gamma}$	$R_{\phi\to K\bar{K}/\rho\pi}$	R_{others}
Preselection	451,924	0.285(1)	$1.86(2)\times10^2$	$5.01(2)\times10^3$	$1.435(8)\times10^3$
χ^2	36,282	0.217(1)	$2.01(3)\times10^2$	$1.13(1)\times10^5$	$3.44(5)\times10^4$
$\Sigma_1^4\lvert\vec{p}_i\rvert$	16,811	0.216(1)	$2.68(5)\times10^2$	$2.21(3)\times10^5$	$6.9(1)\times10^4$
$\cos\theta_b$, $\cos\theta_f$	15,003	0.216(1)	$2.68(5)\times10^2$	$2.21(3)\times10^5$	$6.9(1)\times10^4$
γ conversion	12,198	0.209(1)	$1.11(4)\times10^3$	$2.53(3)\times10^5$	$1.13(3)\times10^5$
PID	4239	0.205(1)	$1.12(4)\times10^3$	$1.02(8)\times10^7$	$5.1(3)\times10^5$

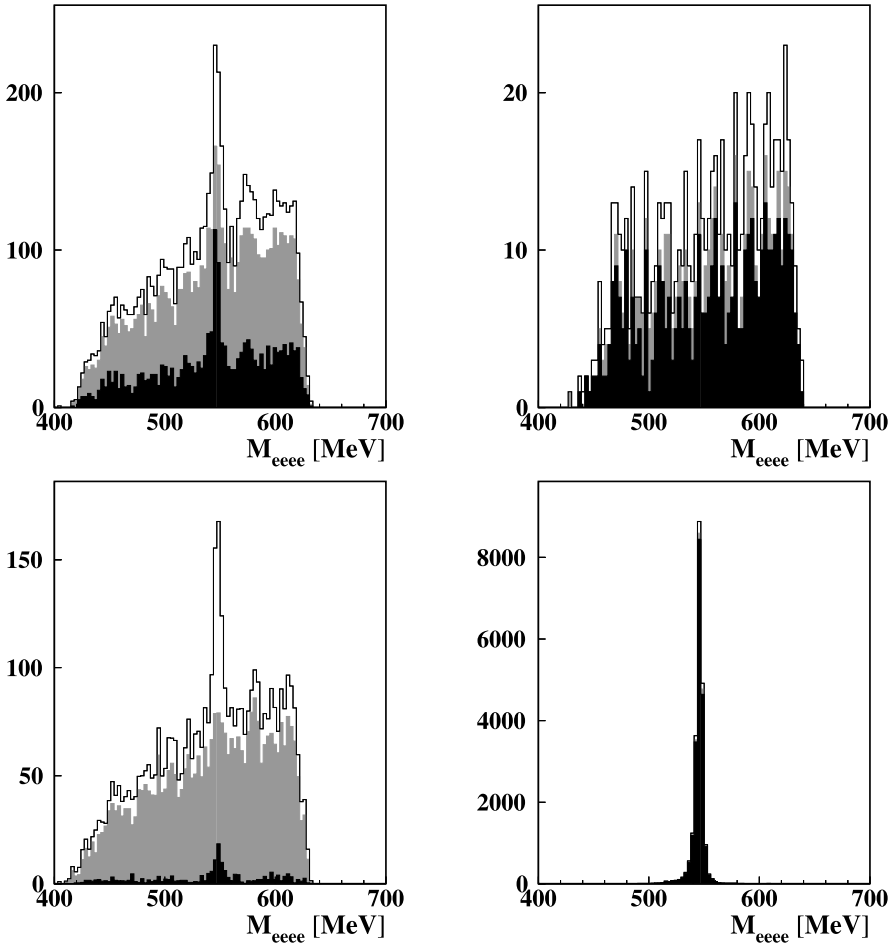

Fig. 2. $M_{e^+e^-e^+e^-}$ distribution after different analysis cuts: white: after the $\sum_1^4|\vec{p}_i|$ and the $\langle\cos\theta\rangle$ cuts; grey: after the cut on photon conversion; black: after the PID requirement. Top left: data; top right: off-peak; bottom left: ϕ background Monte Carlo; bottom right: signal Monte Carlo.

corresponding to $P(\chi^2)=0.12$. The number of signal events is $N(\eta\to e^+e^-e^+e^-)=362\pm29$. The branching ratio has been evaluated according to the formula:

$$\mathrm{BR}\big(\eta\to e^+e^-e^+e^-(\gamma)\big) = \frac{N_{\eta\to e^+e^-e^+e^-(\gamma)}}{N_{\eta\gamma}}\cdot\frac{1}{\epsilon_{\eta\to e^+e^-e^+e^-(\gamma)}} \tag{1}$$

where $N_{\eta\to e^+e^-e^+e^-(\gamma)}$ is the number of signal events and $\epsilon_{\eta\to e^+e^-e^+e^-(\gamma)}$ is the efficiency taken from MC. The number of $\phi\to\eta\gamma$ events, $N_{\eta\gamma}$, has been obtained using the formula $N_{\eta\gamma}=\mathcal{L}\cdot\sigma_{\phi\to\eta\gamma}$, where $\mathcal{L}$ is the integrated luminosity and the cross section $\sigma_{\phi\to\eta\gamma}$ has been evaluated taking into account the ϕ meson line shape on a run by run basis [16]. Inserting all the numbers quoted in Table 2, the value:

$$\mathrm{BR}\big(\eta\to e^+e^-e^+e^-(\gamma)\big)=(2.44\pm0.19_{stat+bckg})\times10^{-5} \tag{2}$$

Table 2
Summary of the numbers used in the master formula (1) for the branching ratio evaluation.

BR inputs	Values
Number of events	362 ± 29
Efficiency $\epsilon_{\eta\to e^+e^-e^+e^-(\gamma)}$	0.205 ± 0.001
Luminosity	(1733 ± 10) nb^{-1}
$e^+e^-\to\phi\to\eta\gamma$ cross section	(41.7 ± 0.6) pb

is obtained, where the error accounts for the uncertainty of the fit result.

The systematic uncertainties due to analysis cuts have been evaluated by applying separately a variation of $\pm1\sigma$ on all variables and re-evaluating the branching ratio. The σ values have been obtained using MC signal events. For the χ^2 variable the cut has been moved by ±500, while the particle identification cut

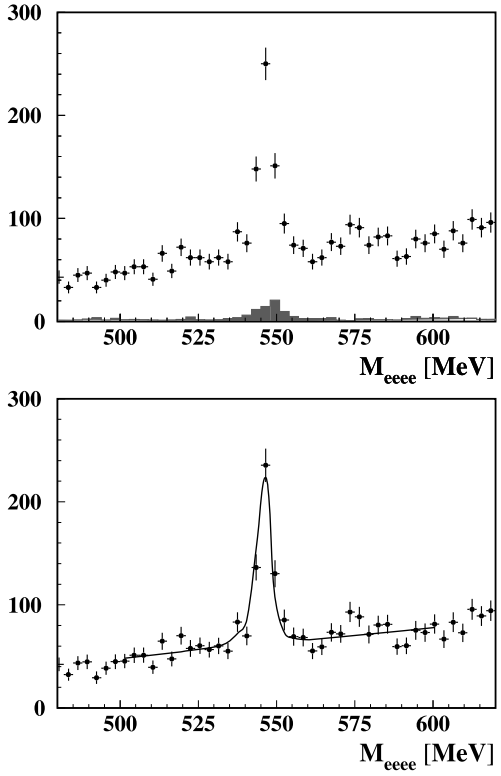

Fig. 3. Top panel: $M_{e^+e^-e^+e^-}$ data distribution at the end of the analysis chain; the expected ϕ background MC shape is shown in grey. Bottom panel: $M_{e^+e^-e^+e^-}$ fit to data after ϕ background subtraction.

Table 3
Summary table of systematic uncertainties.

Source of uncertainty	Relative error
χ^2	$-0.51\%/+2.62\%$
$\langle\cos\theta_b\rangle$ and $\langle\cos\theta_f\rangle$	$-0.04\%/+0.47\%$
$\sum_1^4 \lvert\vec{p}_i\rvert$	$+0.11\%$
γ conversion	$-0.74\%/+2.43\%$
PID	$+1.84\%$
Fit range	$-0.38\%/+1.13\%$
Binning on $M_{e^+e^-e^+e^-}$	$-3.21\%/+0.19\%$
Background slope	$+0.38\%$
Normalization	$\pm1.64\%$
Total	$-3.73\%/+4.53\%$

has been changed by $\pm10\%$. The systematic error on the fit to the $M_{e^+e^-e^+e^-}$ distribution has been evaluated considering:

- the binning of the $M_{e^+e^-e^+e^-}$ histogram, changed from 3 MeV, used as default, to 2 and 4 MeV;
- the $M_{e^+e^-e^+e^-}$ range, enlarged and reduced by 10 MeV on both sides;
- the slope of the e^+e^- continuum background has been fixed to the value obtained from off-peak data fit.

The relative variation of the BR for each source of systematic uncertainty is reported in Table 3. The uncertainty on $N_{\eta\gamma}$ has been added to the systematics in the normalization term. The total error is taken as the quadratic sum of all contributions.

6. Conclusions

Using a sample of 1.7 fb^{-1} collected in the ϕ meson mass region, the first observation of the $\eta \to e^+e^-e^+e^-(\gamma)$ decay has been obtained on the basis of 362 ± 29 events. The corresponding branching ratio is:

$$\mathrm{BR}\big(\eta \to e^+e^-e^+e^-(\gamma)\big) = (2.4 \pm 0.2_{stat+bckg} \pm 0.1_{syst}) \times 10^{-5}. \quad (3)$$

Radiative events slightly modify momentum distribution of the charged particles and have been carefully considered in the efficiency evaluation. As a result, the measured branching ratio is fully radiation inclusive.

Our measurement is in agreement with theoretical predictions, which are in the range $(2.41 - 2.67) \times 10^{-5}$ [2,4–7].

Acknowledgements

We would like to thank J. Bijnens for the useful discussions and for having provided the signal Monte Carlo generator. We thank the DAFNE team for their efforts in maintaining low background running conditions and their collaboration during all data-taking. We want to thank our technical staff: G.F. Fortugno and F. Sborzacchi for their dedication in ensuring efficient operation of the KLOE computing facilities; M. Anelli for his continuous attention to the gas system and detector safety; A. Balla, M. Gatta, G. Corradi and G. Papalino for electronics maintenance; M. Santoni, G. Paoluzzi and R. Rosellini for general detector support; C. Piscitelli for his help during major maintenance periods. This work was supported in part by EURODAPHNE, contract FMRX-CT98-0169; by the German Federal Ministry of Education and Research (BMBF) contract 06-KA-957; by the German Research Foundation (DFG), 'Emmy Noether Programme', contracts DE839/1-4; by the EU Integrated Infrastructure Initiative HadronPhysics Project under contract number RII3-CT-2004-506078; by the European Commission under the 7th Framework Programme through the 'Research Infrastructures' action of the 'Capacities' Programme, Call: FP7-INFRASTRUCTURES-2008-1, Grant Agreement No. 227431; by the Polish Ministery of Science and Higher Education through the Grant No. 0469/B/H03/2009/37.

References

[1] L.G. Landsberg, Phys. Rept. 128 (1985) 301.
[2] C. Jarlskog, H. Pilkuhn, Nucl. Phys. B 1 (1967) 264.
[3] K. Nakamura, et al., Particle Data Group, J. Phys. G 37 (2010) 075021.
[4] T. Miyazaki, E. Takasugi, Phys. Rev. D 8 (1973) 2051.
[5] J. Bijnens, F. Perrsson, arXiv:hep-ph/0106130.
[6] C.C. Lih, J. Phys. G 38 (2011) 065001.
[7] T. Petri, PhD thesis, arXiv:1010.2378 [nucl-th].
[8] R.R. Akhmetshin, et al., CMD-2 Collaboration, Phys. Lett. B 501 (2001) 191.
[9] M. Berlowski, et al., Phys. Rev. D 77 (2008) 032004.
[10] M. Adinolfi, et al., Nucl. Inst. Meth. A 488 (2002) 51.
[11] M. Adinolfi, et al., Nucl. Inst. Meth. A 482 (2002) 364.
[12] M. Adinolfi, et al., Nucl. Inst. Meth. A 492 (2002) 134.
[13] F. Ambrosino, et al., Nucl. Inst. Meth. A 534 (2004) 403.
[14] E. Barberio, Z. Was, Comput. Phys. Commun. 79 (1994) 291.
[15] P. Golonka, Z. Was, Eur. Phys. J. C 45 (2006) 97.
[16] S. Giovannella, S. Miscetti, KLOE note 212, http://www.lnf.infn.it/kloe/pub/knote/kn212.ps, 2006.